

# Indentation Testing of the Optic Nerve Head and Posterior Sclera

Dongyul Chai<sup>1</sup>, Philip Ngai<sup>2</sup>, Bryan E. Jester<sup>1</sup>, Korey M. Reid<sup>1</sup>, Tibor Juhasz<sup>1,3</sup>, James V. Jester<sup>1,3</sup>,  
Don S. Minckler<sup>1</sup>, Donald J. Brown<sup>1</sup>

<sup>1</sup>Gavin Herbert Eye Institute, <sup>2</sup>School of Medicine, <sup>3</sup>Department of Biomedical Engineering  
University of California, Irvine, Irvine, CA, United States

\*<sup>1</sup>dbrown@uci.edu

**Abstract-** The mechanical behavior of the optic nerve head (ONH) and the surrounding sclera play important roles in the development of optic neuropathy. We assessed the indentation behavior of the ONH and the surrounding sclera in unfixed human autopsy eyes from individuals between 27 and 87 years of age. Our testing device utilized a round-tipped 250  $\mu\text{m}$  diameter stainless steel probe to measure the force applied in discrete 50  $\mu\text{m}$  steps from the surface of the tissues to a depth of 400  $\mu\text{m}$ . Thirteen eyes from eight individuals were indented in various locations within and around the ONH and the posterior sclera. Tissue thickness, force and depth were recorded at each position tested. Data was analyzed by evaluating the recorded force as a function of the depth of indentation. The data showed that, for both the sclera and the ONH, the force rose exponentially with increased depth of indentation. Apparent stiffness values were estimated using 2 different equations that assess soft biologic tissues. Results showed that significantly higher levels of force were required with aging to indent the posterior sclera, with a corresponding increase in stiffness values. However, no significant increase in indentation force as a function of age was noted for the ONH. Interestingly, the data suggests that some individuals have relatively large differences in the stiffness between the ONH and the posterior sclera, while others show less difference regardless of age. This data supports the notion that some individuals have relatively softer ONH tissue, and as the sclera becomes stiffer with age, this difference is magnified. This difference may be important in understanding the biomechanical contribution to the individually different susceptibility to glaucoma.

**Keywords-** Optic Nerve Head; Sclera; Biomechanics; Lamina Cribrosa; Aging

## I. INTRODUCTION

Primary open angle glaucoma (POAG) is a primary cause of vision loss in the world [1, 2]. Glaucoma is defined as an irreversible damage to the optic nerve with characteristic changes in the morphology and structure of the optic nerve head (ONH) [3]. Elevations in IOP, a major risk factor for POAG, lead to glaucomatous signs, such as the vertical elongation of the optic cup and thinning of the neuroretinal rim tissue [4]. Elevated IOP has been shown to damage retinal ganglion cell (RGC) axons [5] and block axonal transport at the level of the lamina cribrosa (LC) [6, 7]. The LC is composed of lamellar beams of connective tissue aligned to form 400 to 500 channels or pores where the axons of RGC transverse the sclera [8, 9]. Past studies have demonstrated structural changes in the connective tissue of the LC and the posterior sclera in glaucomatous environments [10-13], while others have investigated the biomechanical behavior of the LC in response to elevated pressure [14, 15]. Most of these biomechanical models suggest that the behavior of the LC is greatly affected by the material properties of the ONH and the posterior sclera [16-18]

A few studies have calculated the elastic moduli of the posterior sclera and the ONH [19, 20] using uniaxial stress-strain measurements to provide an averaged elastic modulus over enucleated specimens, which considers contributions by fibers orientated along the stretched axis. More recently, Eilaghi et al [21] provided stiffness values for regionally defined posterior scleral samples using biaxial tensile measurements. Unfortunately, given the small size of the ONH and its complex structure, differences in the elastic modulus at various regions within the ONH and the posterior sclera have not been established. At the same time, computational models have indicated that the material properties of both the posterior sclera and the LC significantly influence the ONH's response to pressure [18]

The indentation method, which measures indenting force over displacement into the material, has surfaced as an alternative method to assess this material property in biologic materials [22-24]. For this study, we constructed an indentation device and then investigated the forces generated in a stepped indentation within the ONH and the posterior sclera as a function of age, region (superior, inferior, nasal and temporal) and fellow eyes.

## II. MATERIALS AND METHODS

### A. Indentation Device

An indenting force measurement device was built using a 3D positioning control as described in a previous study [25]. In this study, a 250  $\mu\text{m}$  diameter probe with a round tip was attached to the tip of the force transducer, and the z axis actuator was driven by hand (Fig. 1).

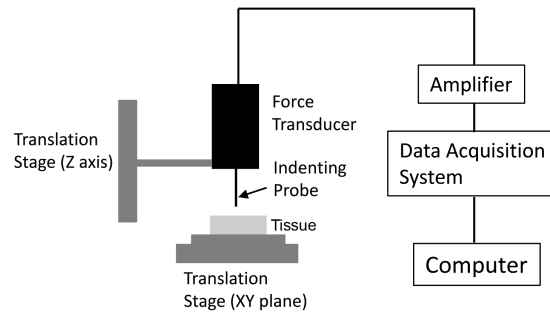


Fig. 1 Schematic of the indentation measurement system. Tissues were located on a XY positioning system composed of translation stages and indented using a round tip probe of 250  $\mu\text{m}$  diameter. The probe was attached to a force transducer fixed on a translation stage placed ninety degrees to the sample. The indenting force from the transducer was recorded by a computer-controlled data acquisition system

### B. Instrument Validation Studies

Polyacrylamide hydrogels were prepared as previously described by Peyton et al [26]. Briefly, acrylamide (Invitrogen, Carlsbad, CA) and bisacrylamide (Sigma-Aldrich, St. Louis, MO) were mixed at various concentrations (8:0.6%, 10: 0.8% and 12.5:1%) and polymerized between glass plates separated by 3 mm spacers with the addition of ammonium persulfate. The resulting 3 mm thick hydrogels were cut into shapes appropriate for testing.

### C. Indentation Measurements

The 25 mm diameter circles of hydrogel were placed on the measuring platform (Fig.1). Force was recorded with displacement of the probe in discrete, 20  $\mu\text{m}$  increments occurring at the center of the hydrogels. Stiffness values were calculated using Eq. 1 [27], referred to as the Hayes equation, which has been used in past studies of soft biologic tissues [28-31]. The values for each measurement were determined by averaging the values calculated over an indenting depth representing 5 – 15% of the gel thickness.

$$E = \frac{1 - \nu^2}{2R\kappa} \frac{F}{\delta} \quad (1)$$

where  $F$ : indenting force,  $\nu$ : Poisson's ratio,  $\delta$ : indenting depth,  $\kappa$ : is a correction factor determined by  $\nu$  and the ratio of  $R$  (radius of indenter) to  $h$  (material thickness)

The value of  $\kappa$  was derived from the table developed by Hayes et al [27] which considers the overall thickness of the hydrogels (3mm), the radius of the indenting tip (125 $\mu\text{m}$ ), and Poisson's ratio of the material. In past studies, most investigators use a range between 0.45 and 0.49 [32, 33] as the assumed value of Poisson's for acrylamide hydrogels. Values for the LC have ranged from 0.49 to 0.5 [34] and 0.46 to 0.5 for the sclera [35]. In all calculations, the assumed value of Poisson's ratio was taken as 0.46 for hydrogels and 0.49 for human tissue. The stiffness value for each acrylamide hydrogel concentration was obtained by averaging the results from 10 independent hydrogels.

### D. Measurement of Compressive Elastic Modulus

Hydrogels were cut into 5  $\times$  5 mm squares and placed on a 13  $\times$  13 mm fixed platform supported by a load cell (Futek, Irvine, CA). As shown in Fig. 2, the gels were compressed at a velocity of 1 mm/min by a computer-controlled moving platform using methods established in prior studies [36, 37]. The stress ( $\sigma$ ) – strain ( $\epsilon$ ) curve was fitted to a polynomial trend line using Excel (Microsoft, Redmond, WA), and the elastic modulus was calculated based on the definition,  $E = d\sigma / d\epsilon$  and determined as the average of 10 independent measurements for each hydrogel concentration.

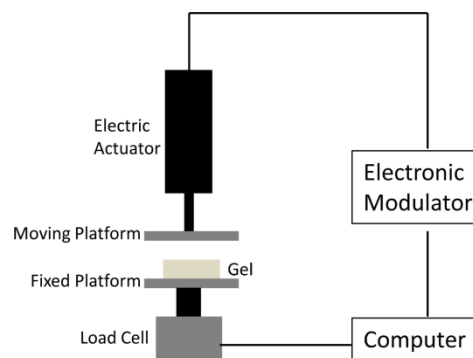


Fig. 2 Schematic of the compressive modulus measurement system. Polyacrylamide hydrogels were located onto a platform fixed on a load cell and compressed by another platform connected to an electric actuator. Compressive force and strain were recorded using a LabVIEW program

## E. Tissue

TABLE 1 CHARACTERISTICS OF EYES USED IN EXPERIMENTS (C; CAUCASIAN)

Subjects	Sex	Age	Race	Time to Preservation (hours)
1	M	27 <sup>a</sup>	N/A	22.25
2	M	27 <sup>b</sup>	N/A	7.3
3	F	56	N/A	7
4	M	62	C	3.3
5	F	63	N/A	10.25
6	F	72	C	21.5
7	M	86	C	10.25
8	F	87	N/A	9

a, b indicate different donors

Thirteen eyes from eight individuals (mean age = 60 +/- 23) (range 27 – 87) were obtained from the San Diego Eye Bank with the approval of the institutional review board and following the tenets established by the Declaration of Helsinki (Table 1). All eyes were preserved within 24 hrs. postmortem and received as whole globes in moist chambers. The Optic nerve was cut flush with the posterior sclera, and the retina and choroid were dissected from the posterior scleral shell (Fig. 3A). The tissue was then cut in a radial pattern to create relaxing incisions to allow flattening of the tissue on the platform, as shown in Fig. 3B. The tissue was fixed to the platform using another board with a central 12.7 mm window, positioning the scleral canal opening in the center of the window (Fig. 3C). The platform with the tissue was then attached to a translation stage, as described in Fig. 1.

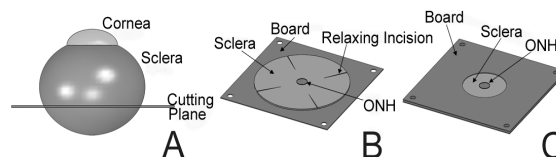


Fig. 3 Preparation of human eye tissue containing the optic nerve head and the posterior sclera. The posterior aspect of the eye was removed along the cutting plane shown in panel A. Relaxing incisions were placed in the posterior sclera to allow a flat mount of the tissue (panel B). A fixing board was placed over the tissue with the ONH centered in the window (panel C)

## F. Measurement of Indenting Force in the ONH and Posterior Sclera

Tissue, attached to the testing device, was indented by a probe in a fixed pattern as demonstrated in Fig. 4. Four positions within the ONH were assessed, representing the superior, inferior, nasal, and temporal regions. Similarly, regions outside the ONH and 4mm away from the canal opening were assessed for the posterior sclera. At each position, the surface contact point was determined by carefully lowering the tip to the tissue surface, and when the signal from the force transducer deviated from zero, the transducer was stopped and its position noted. Tissue thickness at the test point was calculated as the distance between the surface contact point and the surface of the board in Fig. 3B. The indenting probe was lowered into the tissue in discrete 50  $\mu\text{m}$  steps with continuous recording of the transducer force.

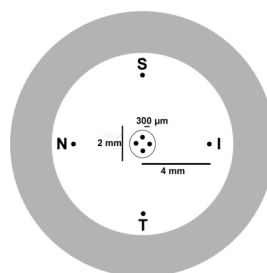


Fig. 4 Indenting pattern on each tissue. Tissue was indented at the positions marked by black dots away from the center of the LC by 300  $\mu\text{m}$  within the ONH and 4 mm within the posterior sclera in each direction. Superior (S), Inferior (I), Nasal (N) and Temporal (T)

The apparent stiffness values from indenting force measurements were estimated using two methods. The first estimate was calculated using the Hayes equation (1), which was also used to calculate values for the hydrogels. Secondly, Eq. 2, referred to as the Hertz equation and commonly used with data derived with atomic force microscopes, was also employed [38],

$$E = \frac{3(1-\nu^2)}{4} \frac{F}{\delta^{3/2} R^{1/2}} \quad (2)$$

where  $\delta$ : indenting depth,  $F$ : indenting force,  $\nu$ : Poisson's ratio,  $R$ : radius of indenter,  $F$ : indenting force

### G. Statistics

The differences in force values at various indentation depths were analyzed using a four way ANOVA (MATLAB, Mathworks, Natick, MA) to account for the variability in measurements by age, region, fellow eyes of the ONH and the posterior sclera. Then, the differences in the averaged values over four regions for each individual eye were also analyzed using a three way ANOVA (MATLAB) to assess for variability between age and fellow eyes. Regression analysis was performed using SigmaStat ver. 3.11 (Systat Software Inc, Point Richmond, CA). P values less than 0.05 were considered significant.

## III. RESULTS

Representative compressive (A) stress – strain curves and the indenting force – strain curve (B) for the 8%, 10%, and 12% acrylamide hydrogels are shown in Fig. 5. The data show that the stress/force at the same level of strain increased with increasing acrylamide concentrations. Stress-strain curves for each hydrogel were fitted to a second order polynomial curve for compressive measurements (Fig. 5A,  $r^2 > 0.99$ ).

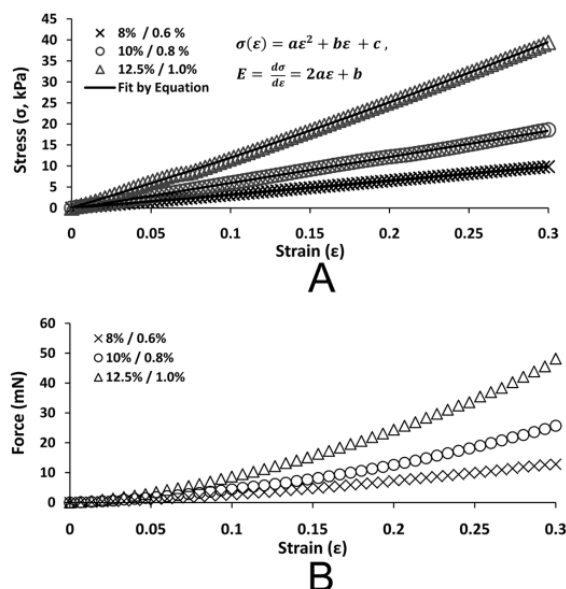


Fig. 5 Experimental results on hydrogels with different concentrations. Stress-strain curves of compressive experiments (A) and force-strain curve of indenting experiment (B). Hydrogels of increasing concentration required larger forces to accomplish similar levels of strain. In panel (A), symbols represent experimental data, and the line through the symbols represents the curve fit to the data. Stress-strain equations and their first derivative were included in panel for compressive experiments. These were used to calculate elastic modulus at specific strains.

TABLE 2 ELASTIC MODULI FROM COMPRESSIVE AND INDENTATION EXPERIMENTS (kPa, MEAN (S.D.))

Acrylamide / Bis-acrylamide	Compressive	Estimated
8% / 0.6 %	30.9 (1.5)	37.1 (4.3)
10% / 0.8 %	64.4 (3.4)	71.3 (6.3)
12.5% / 1.0 %	124.9 (10.1)	125.0 (6.3)

Table 2 shows the stiffness values (mean (S.D.)) of the hydrogels determined by the two different testing methods over 5 – 15% strain. The values obtained by indentation were generally equal to or larger than the values obtained by compression for all acrylamide concentrations. To assess the relationship between the values, linear regression analysis was performed.

As shown in Fig. 6, both testing methods gave similar results, and the only significant difference in values was within the 10% acrylamide group ( $P < 0.05$ ). This data confirmed that the indentation device performed reliably and provided information comparable to compressive testing in uniform hydrogels.

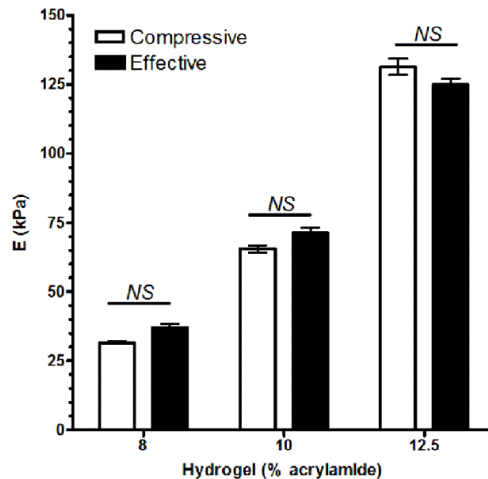


Fig. 6 Compressive (left) and effective modulus (right) of hydrogel at each concentration (NS: not significantly different). Effective modulus values are not significantly different from compressive modulus values at all concentrations.

Fig. 7 shows a representative indenting force measurement profile with a displacement of a 50  $\mu\text{m}$  step. It can be seen that the stepped indentation of the tip led to a rapid increase in force (point a), which then fell to a lower level (point b) that stabilized with time (point c). As this behavior is typical of a viscoelastic response and because the initial slope is rate dependent, forces were recorded after the response became stable and prior to another stepped indentation.

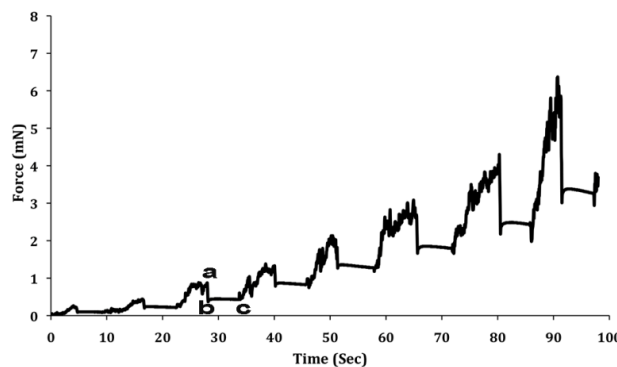


Fig. 7 Representative indentation force over displacement in a 50  $\mu\text{m}$  step. Indenting force increased until probe reached each position (point a) and then fell (point b). Note that indenting force was measured after indenting force stabilized (point c).

Fig. 8 shows the representative material behavior of the tissue, indenting force over indentation depth, for both the posterior sclera and the ONH for a pair of eyes from a 72 year old sample. Much greater force was required to indent the posterior sclera than the ONH for each position tested. In all cases of each eye, the relationship between force and displacement was best characterized as an exponential curve. There was also significant difference in thickness between the scleral and the ONH positions (1047  $\pm$  144 and 1357  $\pm$  172  $\mu\text{m}$ ,  $P < 0.003$ ), which was more variable over the ONH (Fig. 9).

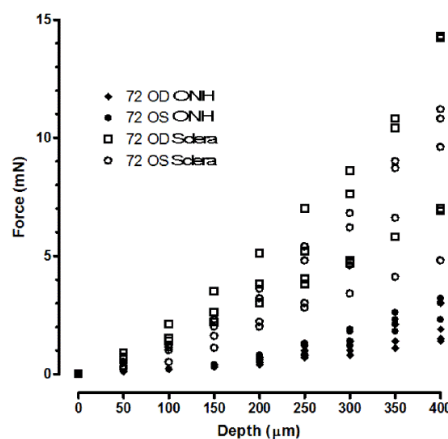


Fig. 8 Indenting force measurements over depth from eyes aged 72. Note that indenting force increases in exponential pattern with larger values at each depth in the sclera than the ONH

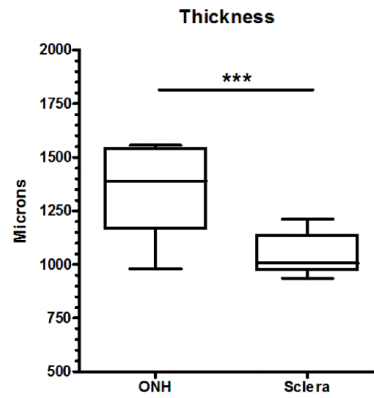


Fig. 9 Thickness of the ONH and the sclera at measuring points from all eyes used in experiment (\*\*\*: P<0.001)

TABLE 3 INDIVIDUAL MEAN AND REGIONAL ESTIMATED E VALUES IN THE ONH AND THE POSTERIOR SCLERA OF EYES USED FOR EXPERIMENTS. RELATIVELY LARGE STANDARD DEVIATION VALUES IN SOME EYES INDICATE SUBSTANTIAL REGIONAL DIFFERENCES IN THE POSTERIOR SCLERA WITHIN AN EYE.

Donor Age	ONH		Posterior Sclera	
	Hayes	Hertz	Hayes	Hertz
27 <sup>a</sup>	10.7 ± 2.45	10.15 ± 2.18	2.13 ± 0.73	1.81 ± 0.64
27 <sup>b</sup>	16.23 ± 8.22	14.14 ± 7.17	5.47 ± 1.35	4.84 ± 1.39
56	35.92 ± 20.33	35.55 ± 21.62	2.8 ± 1.52	2.52 ± 1.52
	36.49 ± 24.91	34.40 ± 22.02	2.97 ± 1.08	2.56 ± 0.57
62	48.68 ± 43.19	46.52 ± 41.15	5.81 ± 1.47	6.31 ± 2.97
	44.82 ± 25.86	43.81 ± 26.91	6.85 ± 3.28	5.32 ± 1.13
63	43.43 ± 21.29	43.32 ± 20.06	3.35 ± 2.55	3.05 ± 2.36
	40.73 ± 26.43	37.76 ± 24.86	2.66 ± 2.12	1.71 ± 1.58
72	77.82 ± 17.78	77.84 ± 16.51	10.8 ± 1.42	9.95 ± 0.8
	51.38 ± 14.54	48.49 ± 14.62	11.74 ± 1.31	10.3 ± 0.69
86	229.45 ± 72.25	210.87 ± 78.70	8.97 ± 7.03	8.5 ± 7.29
87	201.53 ± 93.35	143.89 ± 104.56	15.34 ± 8.15	13.91 ± 7.4
	160.09 ± 66.93	170.95 ± 59.03	19.23 ± 10.51	15.97 ± 7.26

a, b indicate different donors All values indicate kPa ± standard deviation in estimated E values by the Hayes and Hertz models.

Due to the positional variation in tissue thickness, stiffness values were estimated using two methods. One of which considers thickness (Hayes), and the other does not (Hertz). The estimated stiffness values of the posterior and the ONH from all eyes are provided in Tables 3. By four way ANOVA, the estimated values for the posterior sclera were significantly higher than those obtained for the ONH (P<0.001). Additionally, there was significant variation with age (P<0.01) while no

significant differences were noted between left and right eyes from the same individual or regions within a single eye (superior, inferior, nasal, temporal) ( $P > 0.05$ , not shown). This suggests that variations in estimated stiffness values from each measurement point for the same eye tissue could be represented by averaging values over the four regions tested. This was confirmed by a three way ANOVA analysis that showed a difference between the ONH, the sclera, and the age of the individual ( $P < 0.05$ ), regardless of the method used for estimating stiffness.

Fig. 10 shows the estimated stiffness values plotted over age for the posterior sclera (A) and the ONH (B). Spearman rank correlation analysis was performed to assess the relationship between age and apparent stiffness. When considering scleral values, both estimates (Hayes and Hertz) gave  $r$  values of 0.93,  $P < 0.0001$ , suggesting a strong correlation. When considering the values of the ONH, the correlation was less robust with  $r$  values of 0.8 (Hayes) and 0.76 (Hertz),  $P = 0.001$  (Hayes) and 0.002 (Hertz). Linear regression analysis of the log-scaled stiffness values from (A); (B) shows a linear and statistically equivalent trend in both methods for the sclera (C),  $P = 0.95$ ; and, for the ONH (D),  $P = 0.96$ . The goodness of fit was much higher ( $r^2 = 0.93$ ) and with narrower confidence intervals for the scleral values (C) when compared to the estimated stiffness values for the ONH which were highly variable,  $r^2 = 0.51$  (Hayes) and 0.48 (Hertz), without statistical power higher than 80%, suggesting that no reliable regression line could be drawn. These comparisons suggest that the posterior sclera stiffens with age while no clear age effect is present in the ONH.

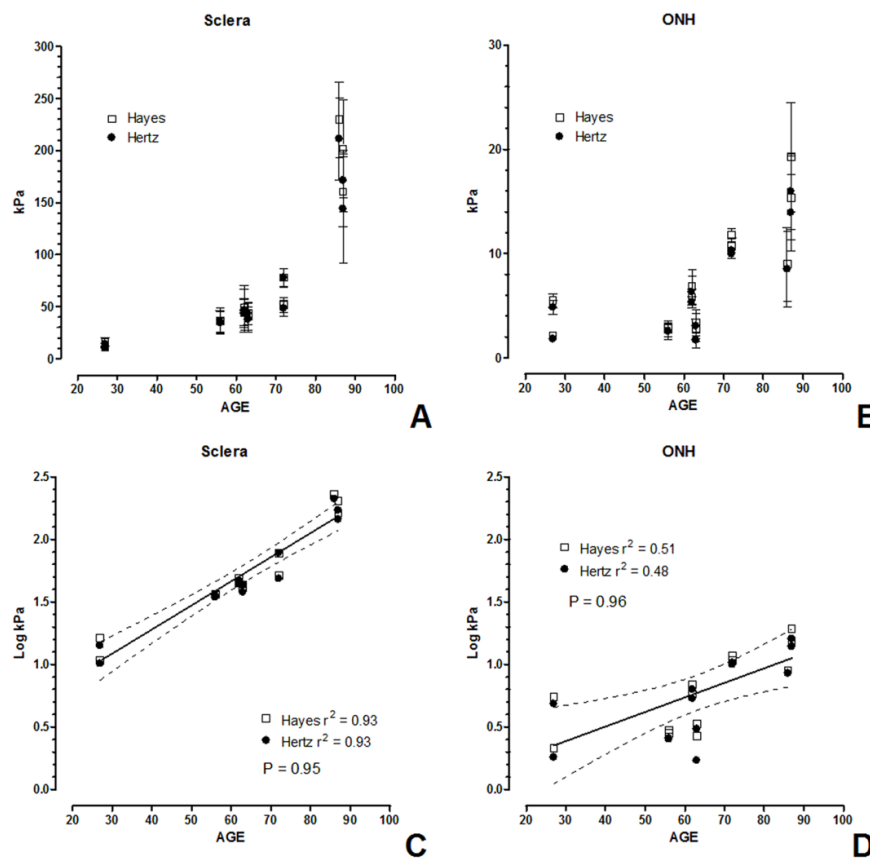


Fig. 10 Estimated stiffness values (mean  $\pm$  SD) over age in the posterior sclera (A), the ONH (B) of all eyes and log-scaled stiffness of sclera (C) and the ONH (D) (dashed line: 95% confidence interval of the line). Regression analysis shows a higher correlation,  $r^2 = 0.93$  (Hayes, Hertz), with a narrow confidence interval between stiffness and age in the sclera (C), with a wider range of confidence interval in the ONH,  $r^2 = 0.51$  (Hayes) and 0.48 (Hertz)

#### IV. DISCUSSION

Our indentation device was constructed to assess the stiffness of human tissues. As such, it was necessary to validate values calculated from indenting force measurements obtained by this device through comparison to those from bulk compression measurements. Polyacrylamide hydrogels were used for this validation in a manner similar to that used in past studies [29]. Reassuringly, high correlations ( $R^2 = 0.93$ ) between stiffness values derived by the constructed device and those derived by conventional compressive measurements were obtained.

In this study, the relative stiffness of the human ocular tissue was estimated from indenting force measurements from the posterior sclera and the ONH without a tensile load. While the normal *in vivo* situation would provide a tensile stress to these tissues, we were unable to provide similar stresses *ex vivo*. However, the indenting force provided by a 250 micron radial tip should reflect the contributions of collagen fibers connected to the measurement point. While various models have been proposed to derive material properties from similar indentation measurements on soft tissues, most rely on the assumption that

the material is uniform and isotropic. Clearly, the tissues tested here are neither uniform nor isotropic and instead represent complex structures. Therefore, the actual deformation of the tissue under the indenting tip could be more complex than simply the depth of the probe into the tissue, making the estimate of strain difficult. Additionally, though relaxing incisions were placed to facilitate mounting the tissue on the testing device (Fig. 3B), the natural curvature of the sclera was bound by the fixing board 12.7mm from the scleral canal and could provide some undefined tensile stress. Therefore, the values reported here must be taken as an indication of the relative stiffness of the tissue, rather than as an estimate of Young's modulus. However, these values are useful when comparing different locations within a tissue or between individuals and have the ability to demonstrate relative behavior of the ONH and the sclera.

We acknowledge that tension is the principal load on the ONH and the posterior sclera, and indentation testing is more comparable to compression than tension. However, compression can also be a significant strain on the ONH, previously estimated to be 5 to 15% strain [39, 40]. As discussed in recent reviews, tensile measurements of soft tissues routinely provide elastic moduli that are orders of magnitude larger than those obtained by indentation [41, 42]. They suggest that tensile measurements are much larger due to the contribution of collagen fiber orientation and water constrained within the tissue. Obviously, stretching or compressing bulk tissue samples requires much larger forces than deforming a localized area [42]. With a small indenting probe, the water is free to move away from the measurement point and where force is not being exerted along the axis of the collagen fibers. Therefore, our data may provide only a few components (among many others) of the mechanical properties within and around the ONH. However, these measurements reflect parameters at defined positions, something not available through standard tensile and compression testing.

The standard deviation of the values presented here for the posterior sclera was quite large, and the variation within a single eye was often as large as the one between individual eyes. This suggests that regional differences in the posterior sclera within a single eye can be as large as the differences between individual eyes, which is in agreement with past studies [19, 21]. However, in spite of the large variation, the data show that the right and left eyes from the same individual are quite similar, and a clear increase in scleral stiffness occurs with increasing age. The values for the ONH were even more variable, and though trending to indicate increasing stiffness with age, the correlation was not strong enough to be consistent regardless of analysis methods. Indeed, the data suggests that some eyes might have a softer ONH, independent of the surrounding sclera and not well correlated with age. This implies that some individuals might have relatively stiffer ONH tissue compared to other individuals, regardless of age.

Most importantly, our study reports the mechanical response in the specific tissues of the optic nerve where glaucomatous damage initially occurs. Elevated IOP applies stresses on the ONH resulting in compression of disc tissues, the LC and likely changes in the geometry of the scleral canal [43-46]. In a recent study, elastic moduli were measured using atomic force microscopy that ranged from 12.7 kPa to 22.0 kPa for the ONH and 101.9 kPa to 221.1 kPa for the posterior sclera from three individuals (64, 72 and 88 years) [47]. These values suggest a difference between ONH and sclera to vary from 5 to 20 fold, entirely consistent with the values we report here. As the magnitude of difference between the sclera and the ONH appeared to be widely different between individuals, this difference may contribute to the pathophysiology of glaucomatous damage, as suggested in the past study [48]. Clearly, further studies are needed to define the distribution of material properties within and around the ONH within a larger population to gain a better biomechanical understanding of the pathology of glaucoma.

#### V. ACKNOWLEDGMENT

This study is supported by NIH grant EY019719, EY018665; Research to Prevent Blindness, Inc and Discovery Eye Foundation.

#### REFERENCES

- [1] S. Kingman, "Glaucoma is second leading cause of blindness globally," *Bulletin of the World Health Organization*, vol. 82, pp. 887-888, 2004.
- [2] S. J. McKinnon, L. D. P. Goldberg, P. J. G. Walt, and T. J. Bramley, "Current Management of Glaucoma and the Need for Complete Therapy," *The American Journal of Managed Care*, vol. 46, pp. S20-S27, 2008.
- [3] P. A. Lin and S. B. Oreng-Nania, U.K., "Management of chronic open-angle glaucoma in the aging US population," *Geriatrics*, vol. 64, pp. 20-26, 2009.
- [4] R. E. Kirsch and D. R. Anderson, "Identification of the glaucomatous disc " *Trans of American Academy of Ophthalmology*, vol. 77, pp. 143-156, 1973.
- [5] R. D. Fechtner and R. N. Weinreb, "Mechanism of Optic-Nerve Damage in Primary Open-Angle Glaucoma," *Survey of ophthalmology*, vol. 39, pp. 23-42, 1994.
- [6] D. S. Minckler, A. H. Bunt, and I. B. Klock, "Autoradiographic and cytochemical ultrastructural studies of axoplasmic transport in monkey optic-nerve head," *Investigative ophthalmology and visual science*, vol. 171, pp. 33-50, 1978.
- [7] M. E. Yablonski and A. Asamoto, "Hypothesis concerning the pathophysiology of optic nerve damage in open angle glaucoma," *Journal of Glaucoma*, vol. 2, pp. 119-127, 1993.
- [8] D. S. Minckler and A. H. Bunt, "Axoplasmic transport in ocular hypotony and papilledema in the monkey," *Arch Ophthalmol*, vol. 95, pp. 1430-6, Aug 1977.
- [9] D. S. Minckler, I. W. McLean, and M. O. Tso, "Distribution of axonal and glial elements in the rhesus optic nerve head studied by electron microscopy," *Am J Ophthalmol*, vol. 82, pp. 179-87, Aug 1976.
- [10] M. R. Hernandez and H. Ye, "Glaucoma: changes in extracellular matrix in the optic nerve head," *Ann Med*, vol. 25, pp. 309-15, Aug 1993.

- [11] H. A. Quigley, R. M. Hohman, E. M. Addicks, R. W. Massof, and W. R. Green, "Morphologic changes in the lamina cribrosa correlated with neural loss in open-angle glaucoma," *Am J Ophthalmol*, vol. 95, pp. 673-91, May 1983.
- [12] M. D. Roberts, V. Grau, J. Grimm, J. Reynaud, A. J. Bellezza, C. F. Burgoyne, et al., "Remodeling of the connective tissue microarchitecture of the lamina cribrosa in early experimental glaucoma," *Invest Ophthalmol Vis Sci*, vol. 50, pp. 681-90, Feb 2009.
- [13] H. Yang, J. C. Downs, C. Girkin, L. Sakata, A. Bellezza, H. Thompson, et al., "3-D histomorphometry of the normal and early glaucomatous monkey optic nerve head: lamina cribrosa and peripapillary scleral position and thickness," *Invest Ophthalmol Vis Sci*, vol. 48, pp. 4597-607, Oct 2007.
- [14] M. E. Edwards and T. A. Good, "Use of a mathematical model to estimate stress and strain during elevated pressure induced lamina cribrosa deformation," *Curr Eye Res*, vol. 23, pp. 215-25, Sep 2001.
- [15] D. B. Yan, F. M. Coloma, A. Metheetairait, G. E. Trope, J. G. Heathcote, and C. R. Ethier, "Deformation of the lamina cribrosa by elevated intraocular pressure," *Br J Ophthalmol*, vol. 78, pp. 643-8, Aug 1994.
- [16] T. Newson and A. El-Sheikh, "Mathematical modeling of the biomechanics of the lamina cribrosa under elevated intraocular pressures," *J Biomech Eng*, vol. 128, pp. 496-504, Aug 2006.
- [17] I. A. Sigal, J. G. Flanagan, I. Tertinegg, and C. R. Ethier, "Modeling individual-specific human optic nerve head biomechanics. Part II: influence of material properties," *Biomech Model Mechanobiol*, vol. 8, pp. 99-109, Apr 2009.
- [18] I. A. Sigal, H. Yang, M. D. Roberts, C. F. Burgoyne, and J. C. Downs, "IOP-induced lamina cribrosa displacement and scleral canal expansion: an analysis of factor interactions using parameterized eye-specific models," *Invest Ophthalmol Vis Sci*, vol. 52, pp. 1896-907, Mar 2011.
- [19] A. Elsheikh, B. Geraghty, D. Alhasso, J. Knappett, M. Campanelli, and P. Rama, "Regional variation in the biomechanical properties of the human sclera," *Experimental Eye Research*, vol. 90, pp. 624-33, May 2010.
- [20] E. Spoerl, A. G. Boehm, and L. E. Pillunat, "The influence of various substances on the biomechanical behavior of lamina cribrosa and peripapillary sclera," *Invest Ophthalmol Vis Sci*, vol. 46, pp. 1286-90, Apr 2005.
- [21] A. Eilaghi, J. G. Flanagan, I. Tertinegg, C. A. Simmons, G. W. Brodland, and C. R. Ethier, "Biaxial mechanical testing of human sclera," *Journal of Biomechanics*, vol. 43, pp. 1696-1701, Jun 18 2010.
- [22] M. Geerligts, L. van Breemen, G. Peters, P. Ackermans, F. Baaijens, and C. Oomens, "In vitro indentation to determine the mechanical properties of epidermis," *J Biomech*, vol. 44, pp. 1176-81, Apr 7 2011.
- [23] J. A. Last, P. Russell, P. F. Nealey, and C. J. Murphy, "The applications of atomic force microscopy to vision science," *Invest Ophthalmol Vis Sci*, vol. 51, pp. 6083-94, Dec 2010.
- [24] V. T. Nayar, J. D. Weiland, and A. M. Hodge, "Macrocompression and nanoindentation of soft viscoelastic biological materials," *Tissue Eng Part C Methods*, vol. 18, pp. 968-75, Dec 2012.
- [25] M. Winkler, D. Chai, S. Kriling, C. J. Nien, D. J. Brown, B. Jester, et al., "Nonlinear optical macroscopic assessment of 3-D corneal collagen organization and axial biomechanics," *Invest Ophthalmol Vis Sci*, vol. 52, pp. 8818-27.
- [26] S. R. Peyton and A. J. Putnam, "Extracellular matrix rigidity governs smooth muscle cell motility in a biphasic fashion," *J Cell Physiol*, vol. 204, pp. 198-209, Jul 2005.
- [27] W. C. Hayes, L. M. Keer, G. Herrmann, and L. F. Mockros, "A mathematical analysis for indentation tests of articular cartilage," *J Biomech*, vol. 5, pp. 541-51, Sep 1972.
- [28] J. W. Klaesner, P. K. Commean, M. K. Hastings, D. Zou, and M. J. Mueller, "Accuracy and reliability testing of a portable soft tissue indenter," *IEEE Trans Neural Syst Rehabil Eng*, vol. 9, pp. 232-40, Jun 2001.
- [29] I. Levental, K. R. Levental, E. A. Klein, R. Assoian, R. T. Miller, R. G. Wells, et al., "A simple indentation device for measuring micrometer-scale tissue stiffness," *J Phys Condens Matter*, vol. 22, p. 194120, May 19 2010.
- [30] M. H. Lu, W. N. Yu, Q. H. Huang, Y. P. Huang, and Y. P. Zheng, "A Hand-Held Indentation System for the Assessment of Mechanical Properties of soft Tissues In Vivo," *IEEE Trans Instrumentation and Measurement*, vol. 58, pp. 3079-3085, 2009.
- [31] J. A. M. A. Soons, J. and J. J. J. Dircks, "Elasticity modulus of rabbit middle ear ossicles determined by a novel micro-indentation technique," *Hearing Research*, vol. 263, pp. 33-37, 2010.
- [32] U. Chippada, B. Yurke, and N. A. Langrana, "Simultaneous determination of Young's modulus, shear modulus, and Poisson's ratio of soft hydrogels," *Journal of Materials Research*, vol. 25, pp. 545-555, Mar 2010.
- [33] T. Takigawa, Y. Morino, K. Urayama, and T. Masuda, "Poisson's ratio of polyacrylamide (PAAm) gels," *Polymer Gels and Networks*, vol. 4, pp. 1-5, 1996.
- [34] S. L. Woo, A. S. Kobayash, C. Lawrence, and W. A. Schlegel, "Mathematical-Model of Corneo-Scleral Shell as Applied to Intraocular Pressure-Volume Relations and Applanation Tonometry," *Annals of Biomedical Engineering*, vol. 1, pp. 87-98, 1972.
- [35] J. L. Battaglioli and R. D. Kamm, "Measurements of the Compressive Properties of Scleral Tissue," *Investigative Ophthalmology & Visual Science*, vol. 25, pp. 59-65, 1984.
- [36] I. Krupa, T. Nedelcev, D. Racko, and I. Lacik, "Mechanical properties of silica hydrogels prepared and aged at physiological conditions: testing in the compression mode," *Journal of Sol-Gel Science and Technology*, vol. 53, pp. 107-114, Jan 2010.
- [37] Y. Yildiz, N. Uyanik, and C. Erbil, "Compressive elastic moduli of poly(N-isopropylacrylamide) hydrogels crosslinked with poly(dimethyl siloxane)," *Journal of Macromolecular Science Part a-Pure and Applied Chemistry*, vol. 43, pp. 1091-1106, 2006.
- [38] W. R. Bowen, R. W. Lovitt, and C. J. Wright, "Application of atomic force microscopy to the study of micromechanical properties of biological materials," *Biotechnology Letters*, vol. 22, pp. 893-903, 2000.
- [39] J. Albon, P. P. Purslow, W. S. S. Karwatowski, and D. L. Easty, "Age related compliance of the lamina cribrosa in human eyes," *British Journal of Ophthalmology*, vol. 84, pp. 318-323, Mar 2000.
- [40] I. A. Sigal, J. G. Flanagan, I. Tertinegg, and C. R. Ethier, "Predicted extension, compression and shearing of optic nerve head tissues," *Experimental Eye Research*, vol. 85, pp. 312-322, Sep 2007.
- [41] M. J. Buehler, "Nature designs tough collagen: Explaining the nanostructure of collagen fibrils," *Proceedings of the National Academy of Sciences of the United States of America*, vol. 103, pp. 12285-12290, Aug 15 2006.
- [42] C. T. McKee, J. A. Last, P. Russell, and C. J. Murphy, "Indentation Versus Tensile Measurements of Young's Modulus for Soft Biological Tissues," *Tissue Engineering Part B-Reviews*, vol. 17, pp. 155-164, Jun 2011.
- [43] H. Mochizuki, A. G. Lesley, and J. D. Brandt, "Shrinkage of the scleral canal during cupping reversal in children," *Ophthalmology*, vol.

- 118, pp. 2008-13, Oct 2011.
- [44] I. A. Sigal and J. L. Grimm, "A few good responses: which mechanical effects of IOP on the ONH to study?," *Invest Ophthalmol Vis Sci*, vol. 53, pp. 4270-8, 2012.
- [45] H. Yang, H. Thompson, M. D. Roberts, I. A. Sigal, J. C. Downs, and C. F. Burgoyne, "Deformation of the early glaucomatous monkey optic nerve head connective tissue after acute IOP elevation in 3-D histomorphometric reconstructions," *Invest Ophthalmol Vis Sci*, vol. 52, pp. 345-63, Jan 2011.
- [46] A. J. Bellezza, C. J. Rintalan, H. W. Thompson, J. C. Downs, R. T. Hart, and C. F. Burgoyne, "Anterior scleral canal geometry in pressurised (IOP 10) and non-pressurised (IOP 0) normal monkey eyes," *Br J Ophthalmol*, vol. 87, pp. 1284-90, Oct 2003.
- [47] C. Braunsmann, C. M. Hammer, J. Rheinlaender, F. E. Kruse, T. E. Schaffer, and U. Schlotzer-Schrehardt, "Evaluation of lamina cribrosa and peripapillary sclera stiffness in pseudoexfoliation and normal eyes by atomic force microscopy," *Invest Ophthalmol Vis Sci*, vol. 53, pp. 2960-7, 2012.
- [48] R. C. Zeimer, in *Optic Nerve in Glaucoma*, D. SM, Ed., ed Amsterdam, The Netherlands: Kugler Publications, 1995, pp. 107-121.